Propagation in the Off Center *E*-Plane Dielectrically Loaded Waveguide

NIKOLAI EBERHARDT

Abstract—**Rectanuglar waveguides containing a full height lossless dielectric slab in arbitrary positions are theoretically treated. Numerical data about the cutoff frequencies of the three lowest TE-modes in the case of loading with alumina are presented. A graphical method is developed to determine cutoff frequencies for other dielectric constants as well. Graphs are given to determine the propagation constant and its frequency dependence. Figures of some characteristic mode patterns are added. A possible application to dissipative filters and frequency separators is discussed.**

RECTANGULAR waveguides loaded with a full height dielectric slab as shown in Fig. 1 are used in devices such as dielectric phase shifters, electronically variable ferrite phase shifters, isolators, and filters. The special case of the slab located in center of the guide has been thoroughly treated by Vartanian, Ayres, and Helgesson [1]. Other approaches are known, [3]–[5], [8] but are restricted to small values of ϵ or special slab positions. In some of the mentioned devices, configurations have to be used where the slab is located off center. This case has not been solved so far. There is no analytic solution. Having the four parameters: slab thickness, position, dielectric constant, and frequency, the problem resists even numerical presentation on a limited number of pages. Nevertheless there is urgent need to have more theoretical background for certain design procedures. Moreover a better knowledge of the mode patterns and their behavior is of great value to the designer of waveguide devices.

An interesting result of this investigation is that in the case of a thin dielectric slab of high permittivity there exists a sharp critical frequency above which almost all power propagates inside of the dielectric material. Below this frequency, however, the field is approximately identical with that of the empty guide. The critical frequency approximately coincides with the cutoff frequency of a dielectric mode inside of the slab. This effect has been used by the author to construct dissipative high-pass filters, band absorption filters, and harmonic filters [9].

General Theory

The basic approach is straightforward and appears well referred [7]. In order to obtain normalized results the following parameters are introduced. The dimensions a, c, d may be taken from Fig. 1:

ϵ = relative dielectric constant of the slab.
c/a = normalized slab thickness.

Manuscript received January 26, 1966; revised December 7, 1966. This work was done under contract to Bell Telephone Labs., Allentown, Pa.

The author is with the Dept. of Electrical Engineering, Lehigh University, Bethlehem, Pa.

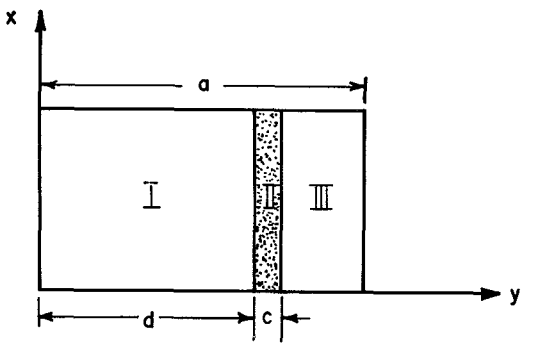

Fig. 1. Cross section of a dielectrically loaded waveguide.

$ka = \omega\sqrt{\mu_0\epsilon_0}\ a$ = normalized frequency.
$e = (a-c)/2d$ = position parameter.

If the slab is located in the center of the guide e becomes 1; it decreases if the slab is moved toward the right wall; and $e = \frac{1}{2}$ if the right wall is touched.

The unbounded space propagation constant is $\gamma_0 = j\omega\sqrt{\mu_0\epsilon_0}$. It is seen that the following electric field is sufficient to match all boundary conditions

$$\text{In region I:}\quad E_x = \sin \beta_y y. \tag{1a}$$

$$\text{In region II:}\quad E_x = C\cos \beta_y' y + D \sin \beta_y' y. \tag{1b}$$

$$\text{In region III:}\quad E_x = B \sin \beta_y (a - y). \tag{1c}$$

Higher "TE_{n0}-modes" are described by this approach as well, if β_y and β_y' are chosen so that E_x passes through zero several times between $y=0$ and $y=a$. We will call a mode the distorted TE_{10}-mode if the E_x-field is zero only at $y=0$ and $y=a$. Similarly a distorted TE_{n0}-mode is present if there are $n-1$ zero points inside that interval. It is found to be advantageous to normalize the transverse propagation constants

$$\beta_y = \frac{p}{d}$$

$$\beta_y' = \frac{2q}{c}.$$

p and q now determine β_y and β_y'. Where possible the same terminology is used as by Vartanian, Ayres, and Helgesson [1], so that this theory in the special case of $e=1$ becomes identical with the theory in reference [1].

Assuming $\mu=1$ everywhere; $\epsilon=1$ in regions I, III; $\epsilon>1$ in region II, and introducing (1a) or (1c) into Helmholtz's equation we find the characteristic equation

$$\left(\frac{p}{d}\right)^2 = \gamma^2 + \omega^2\epsilon_0\mu_0. \tag{2a}$$

Equation (1b) yields similarly:

$$\left(\frac{2q}{c}\right)^2 = \gamma^2 + \omega^2\epsilon\epsilon_0\mu_0. \tag{2b}$$

Magnetic and electric boundary conditions at the air dielectric interfaces yield four equations. With equation (2) they determine:

$$D = \sin p \sin \frac{q}{er} + \frac{per}{q} \cos p \cos \frac{q}{er} \tag{3}$$

$$C = \sin p \cos \frac{q}{er} - \frac{per}{q} \sin \frac{q}{er} \cos p \tag{4}$$

$$B = \frac{C \cos q\frac{1}{er} + 2 + D \sin q\frac{1}{er} + 2}{\sin p\,(2e-1)} \tag{5}$$

$$q^2 = (pre)^2 + \frac{\epsilon - 1}{4}\left(\frac{c}{a}\right)^2 (ka)^2 \tag{6}$$

$$\tan 2q = -\frac{per}{q}\,\frac{\tan p\,(2e-1) + \tan p}{\frac{per}{q} - \tan p \tan p\,(2e-1)} \tag{7}$$

where

$$r = \frac{\frac{c}{a}}{1 - \frac{c}{a}}.$$

Equations (6) and (7) determine the normalized eigenvalues p and q, which are the key to all previous field expressions. It is impossible to find an explicit solution because of the transcendental nature of (7). For a slab at the center ($e=1$), (6) and (7) simplify to the set derived by Vartanian et al. [1]. Their higher-order solutions describe the fields of the distorted TE_{n0}-modes. Some numerical results will be presented later on.

Cutoff Frequency

At the cutoff frequency γ has to approach zero. Thus (2a) and (2b) result in $p_c = q_c/er\sqrt{\epsilon}$, where the subscript indicates that p and q are taken at cutoff frequency. Together with (7) this yields another transcendental equation

$$\tan 2er\sqrt{\epsilon}\,p_c = -\frac{1}{\sqrt{\epsilon}}\,\frac{\tan p_c(2e-1) + \tan p_c}{\frac{1}{\epsilon} - \tan p_c \tan p_c(2e-1)}. \tag{8}$$

If this equation could be solved in terms of p_c the cutoff frequency would be determined by (2a) as

$$(ka)_c = p_c\frac{a}{d} \quad \text{or by}$$

$$\frac{\lambda_c}{a} = \frac{2\pi}{p_c}\cdot\frac{d}{a}, \tag{9}$$

the normalized cutoff wavelength.

Obviously higher-order solutions of (8) determine the cutoff wavelengths of the distorted TE_{n0}-modes with $n>1$.

The author has set up an iteration process for the computer to solve for as many higher cutoff wavelengths as desirable. The complete graphical presentation of a function of the three variables c/a, e, ϵ is out of the format of this article. In Figs. 2 through 4, the three largest cutoff wavelengths for $\epsilon=9.3$ are plotted, this corresponds to the widely used Al_2O_3 (Alumina) as the dielectric material.

Graphical Solution for Cutoff Frequency

A graphical solution of (8) can be based on the fact that there is close relationship to the trigonometric identity as

$$\tan(\alpha+\beta) = \frac{\tan\alpha + \tan\beta}{1 - \tan\alpha\tan\beta}$$

shown in Fig. 5. Along the tangent f to a unit circle two distances h and l are plotted. The distance $1/\sqrt{\epsilon}$ is plotted on the diameter. The angles α and β thus are related to those distances by $h=1/\sqrt{\epsilon}\tan\beta$ and $l=1/\sqrt{\epsilon}\tan\alpha$. The angle $\alpha+\beta$, according to the above identity, must have the following relation to l and h

$$\tan(\alpha+\beta) = \frac{\sqrt{\epsilon}\,l + \sqrt{\epsilon}\,h}{1 - \epsilon lh} = \frac{1}{\sqrt{\epsilon}}\,\frac{l+h}{\frac{1}{\epsilon} - l\cdot h}.$$

We only need to construct

$$l = \tan p_c \quad \text{and} \quad h = \tan p_c(2e-1),$$

as is easily done by plotting the arguments as angles into the unit circle, and have

$$\tan(\alpha+\beta) = \frac{1}{\sqrt{\epsilon}}\cdot\frac{\tan p_c + \tan p_c(2e-1)}{\frac{1}{\epsilon} - \tan p_c \tan p_c(2e-1)}$$

$$= -\tan(2er\sqrt{\epsilon}\,p_c)$$

$$= \tan(180^\circ - 2er\sqrt{\epsilon}\,p_c).$$

Thus, $2er\sqrt{\epsilon}\,p_c = A$ can be measured as the supplementary angle between the lines n and m. The chart in Fig. 6 can be used as a graphical aid for this construction. The procedure is straightforward:

1) Select ϵ, e, and a tentative value for p_c.
2) Plot the straight line r using the p-scale [1] which is just a clockwise angle scale in radians and find the intersection L with the tangent f.
3) Plot the straight line s using the net chart consisting of the scales [2], [3] and find the intersection H. (With the net chart the angle $p_c(2e-1)$ is constructed.)
4) Find the point E on the ϵ-scale [4] and draw the straight lines EH and EL. Using a compass, transfer the angle A to measure it with scale [1].

Alteration

If the lines r or s intersect too far out with f, take the tangent g instead of f and use the ϵ-scale (5) instead of (4). Otherwise proceed as before. This alteration is based on

the fact that a similar trigonometric identity exists for the cotangent function.

After $A=2ep_cr\sqrt{\epsilon}$ is determined, the necessary slab thickness c/a and the related cutoff wavelength follow from

$$\frac{c}{a}=\frac{r}{1+r} \quad \text{with} \quad r=\frac{A}{2e\sqrt{\epsilon}\,p_c}$$

and (9).

A nomogram (Fig. 7) has been developed to solve the problem purely graphically. Draw a straight line through ϵ and A on the proper scales and find intersection F with the p_c scale. Draw a straight line through p_c and e on the proper scales and find intersection G with line b. Draw a straight line through p_c and e on the proper scales and find intersection G with line b. Draw a straight line through F and G and read c/a and λ_c/a at the intersections of this line with the scales.

The following example is shown: $\epsilon=9.2$, $e=0.8$, and $p_c=1.08$ yield $A=0.55$ with the aid of the circular chart. Going into the nomogram with these values results in $\lambda_c/a=3.25$ and $c/a=0.1$. The described method has the disadvantage that p_c has to be chosen initially. Thus, it is not known which λ_c/a or which c/a will result. However, some complete set of correlated values ϵ, e, c/a, λ_c/a will be obtained. By varying p_c one soon ends up within the range of particular interest.[1] Higher mode cutoff wavelengths can be obtained by gradually increasing p_c until the same c/a will result.

Fortunately the construction works faster than it can be described in words. The reader is invited to check a few of the computed data in Figs. 2 through 4 before he tries to solve for other dielectric constants.

Propagation Constant

Equations (2a) and (2b) are dispersion relations. They differ from the analogous relationship for the empty (or completely filled) waveguide by the fact that the left-hand side is frequency dependent through p and q. From (2b) we obtain

$$\beta^2=\omega^2\epsilon\epsilon_0\mu_0-\left(\frac{2q}{c}\right)^2. \tag{10}$$

Equations (6) and (7) indicate that q and consequently γ will depend on the four parameters: (ka), e, c/a, and ϵ. However, for graphical presentation it is possible to reduce the number of parameters to three. ϵ and (ka) appear only in (6) and here in the combination $(\epsilon-1)\cdot(ka)^2$. Therefore we define

$$F=ka\sqrt{\epsilon-1} \tag{11}$$

and consider q to be a function of F, e, and c/a. In Figs. 8 through 10, q and p have been plotted as a function of F and e for three different slab thicknesses c/a. Therefore, p and q can be obtained for every combination of ϵ, ka, and e. The propagation constant then follows directly from (10).

Some Characteristic Field Patterns and Possible Applications

After p and q are known every field component can be calculated from the equations in the first paragraph. Some typical field configurations have been plotted in Figs. 11 through 14 to provide a better understanding of such waves. It should be noted that p always becomes real at the cutoff frequency. A real p means a sinusoidal y-dependence of the fields in the air space. At higher frequencies however, and if the dielectric loading is strong enough, p turns imaginary and the fields in the air space decay fast according to hyperbolic sin and cos functions. At the transition point, where $p=0$, there is a linear increase.

All fields have been normalized to equal power flow. The normalized field strength E_x is dimensionless and is connected with the true field strength E_x' by the equation

$$E_x'=\left(\frac{4\eta}{ab}P\right)^{1/2}\cdot E_x \tag{12}$$

where η is the intrinsic impedance, a and b are the waveguide dimensions, and P is the transmitted power. The normalization procedure is described in Appendix I.

Of particular interest is the case of a thin slab with high dielectric constant touching the wall, as shown in Fig. 14. Between $F=100$ and $F=110$ there is a sudden increase of the field strength within the slab. Simultaneously the field in the left part of the space drops to virtually zero. The critical value of F is about 105. The physical reason for this remarkable change within ten percent bandwidth is to be seen in the cutoff behavior of the dielectric waveguide which is formed by the slab. It turns out that at F_{crit} the slab thickness c is just equal to $\lambda/4$ of a TEM-wave traveling in y-direction. Thus, F_{crit} apparently describes the cutoff frequency of a mode that is built up by multiple reflections of a TEM-wave between the right surface of the dielectric material (short-circuited end) and the left surface (approximately open end). An outline of the theory of such dielectric modes is included in Appendix II. According to this mechanism F_{crit} can be directly expressed in terms of c/a

$$F_{crit}\approx\frac{\pi}{2\frac{c}{a}}. \tag{13}$$

If the dielectric material is lossy, frequencies above F_{crit} will be attenuated much more strongly than those below, resulting in a simple dissipative low-pass filter.[2]

[1] The following approximation may be used to determine an initial value of p_c if λ_c/a is given and c/a is to be determined

$$p_c\approx\frac{1}{\frac{\lambda_c}{a}\cdot e}.$$

This is implied in (9) if $c\ll a$.

[2] Various filters of this type have been successfully operated by the author.

Another possible application would be frequency separation. Coupling apertures in the dielectric region will couple only to the high frequency. Whether or not there will be coupling to high frequencies in the center of the guide will depend on the presence of higher modes. It is interesting to note that, if the slab is removed from the wall, the critical frequency of the TE_{20} and TE_{30} mode is approximately given by

$$F_{\text{crit},20} \approx \frac{\pi}{\frac{c}{a}} \tag{14a}$$

$$F_{\text{crit},30} \approx \frac{2\pi}{\frac{c}{a}} . \tag{14b}$$

These frequencies correspond to $c=\lambda/2$ and $c=\lambda$ of a transverse TEM-wave and are the cutoff frequencies of higher dielectric modes. This suggests the conclusion that above F_{crit} the propagation occurs mainly in a dielectric mode which is composed by multiple reflections of transverse TEM-waves at the dielectric surfaces. Near F_{crit} the surfaces act as open circuits.

The relatively fast transition from hyperbolic to sinusoidal fields near F_{crit} is apparently enforced by the resonance behavior of the dielectric slab at the dielectric cutoff.

But $F_{\text{crit},20}$ is the lowest possible dielectric resonance between two air to dielectric interfaces. Therefore, no fast transition can occur in the case of the TE_{10}-mode with the slab removed from the wall. Nevertheless the electric field strength at the interfaces will gradually decrease with increasing frequency, because, according to Appendix II, the boundary acts as a short circuit at high frequencies.[3]

[3] The transition may be still sharp enough for the construction of harmonic frequency separators as in U. S. Patent 2 963 661 by H. Seidel.

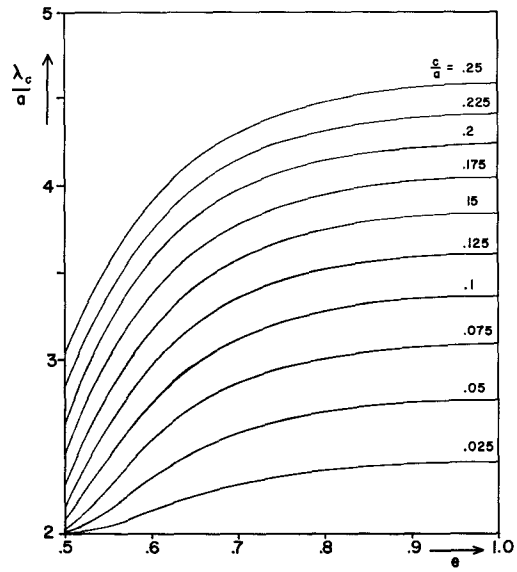

Fig. 2. Cutoff wavelength of the TE_{10}-mode, $\epsilon=9.3$.

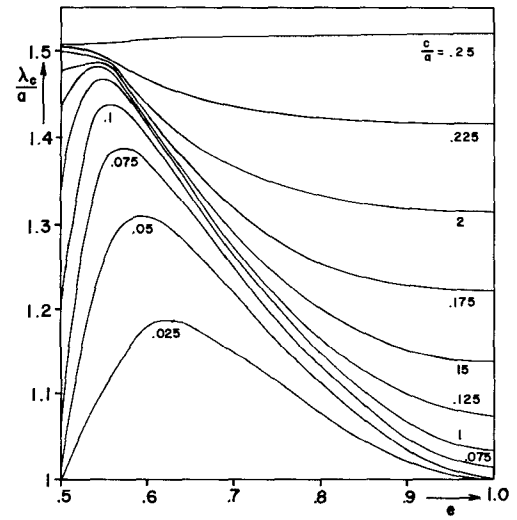

Fig. 3. Cutoff wavelength of the TE_{20}-mode, $\epsilon=9.3$.

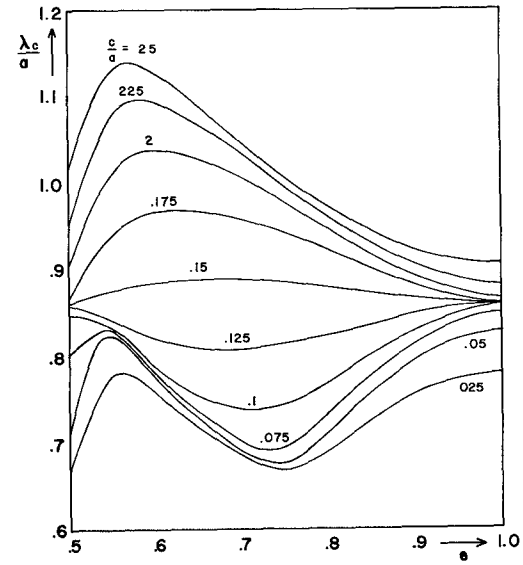

Fig. 4. Cutoff wavelength of the TE_{30}-mode, $\epsilon=9.3$.

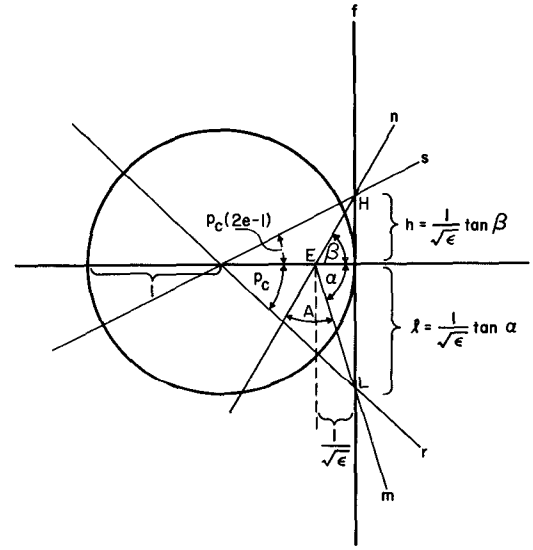

Fig. 5. Graphical representation of (8).

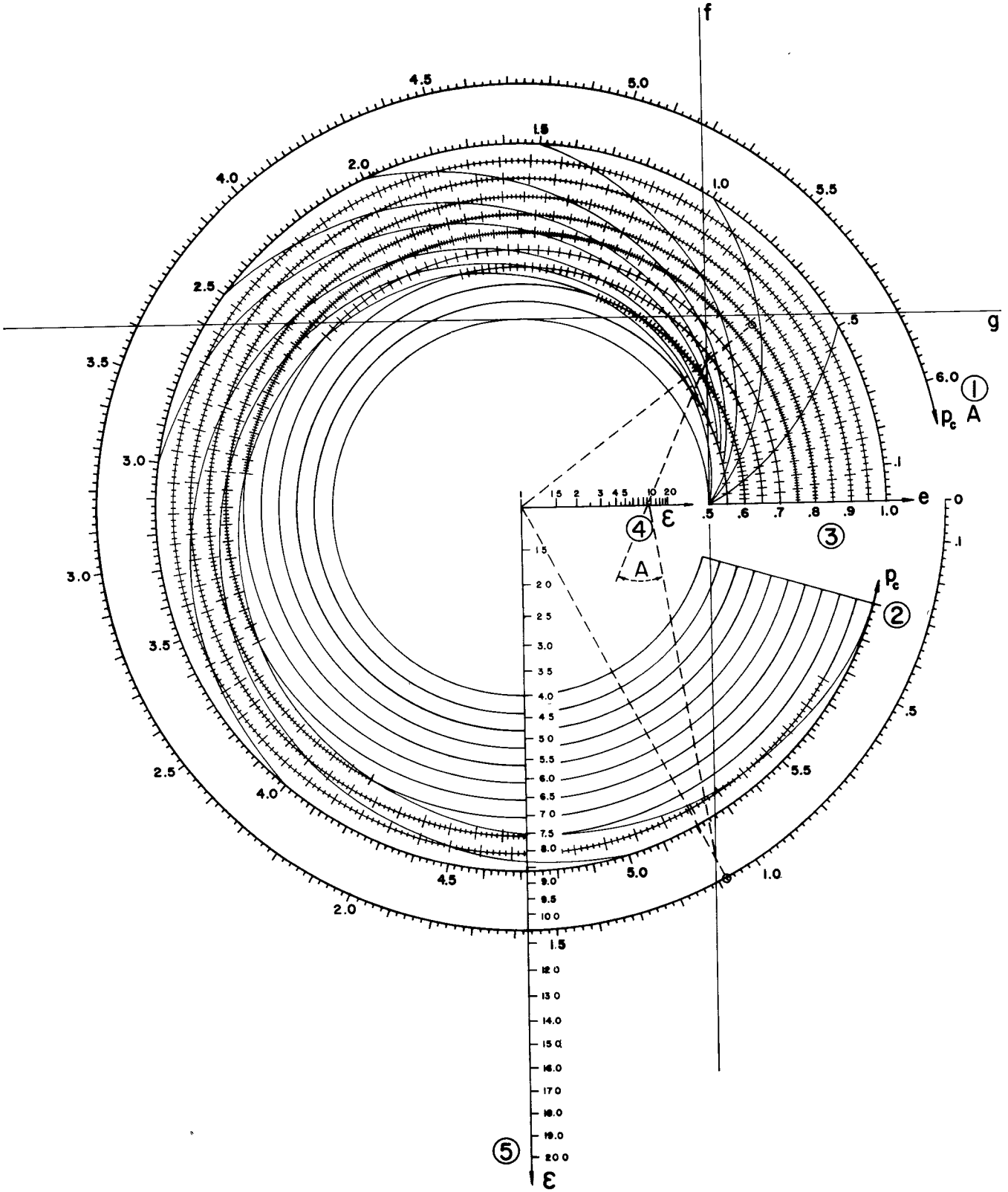

Fig. 6. Chart of (8).

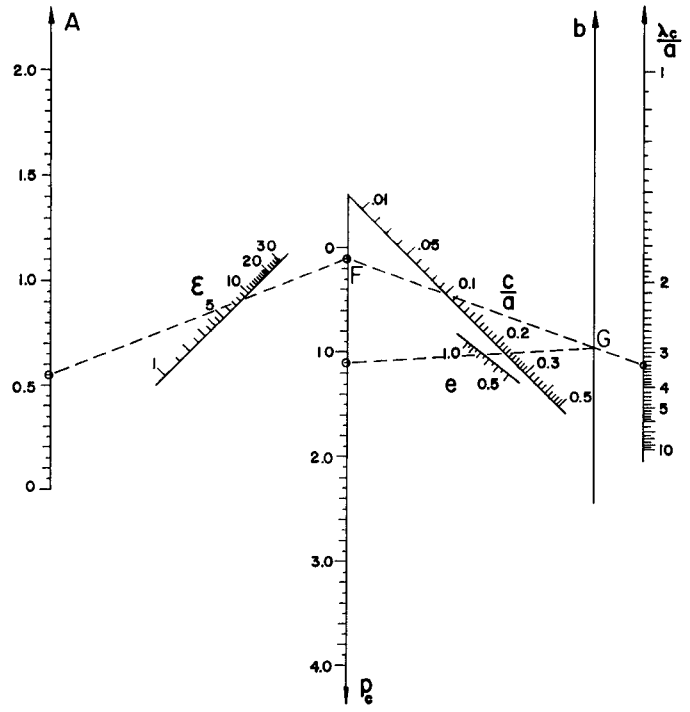

Fig. 7. Nomogram for c/a and λ_c/a.

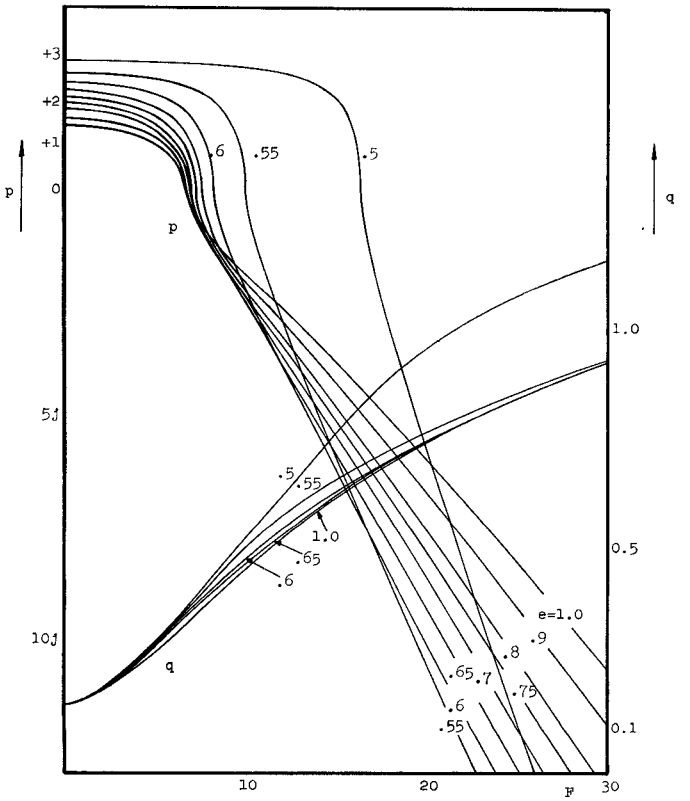

Fig. 8. p and q as a function of F and e; $c/a=0.1$.

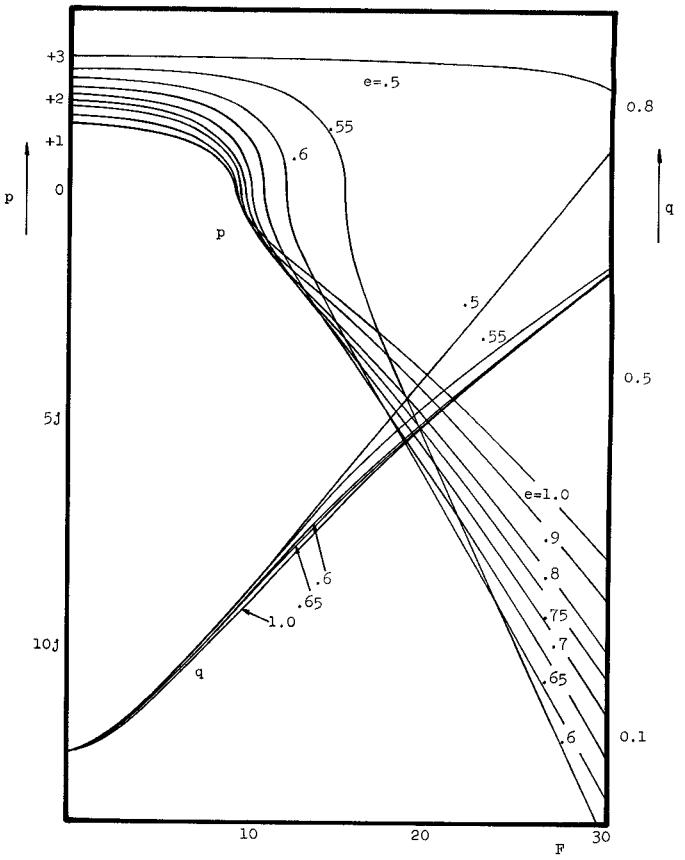

Fig. 9. p and q as a function of F and e; $c/a=0.05$.

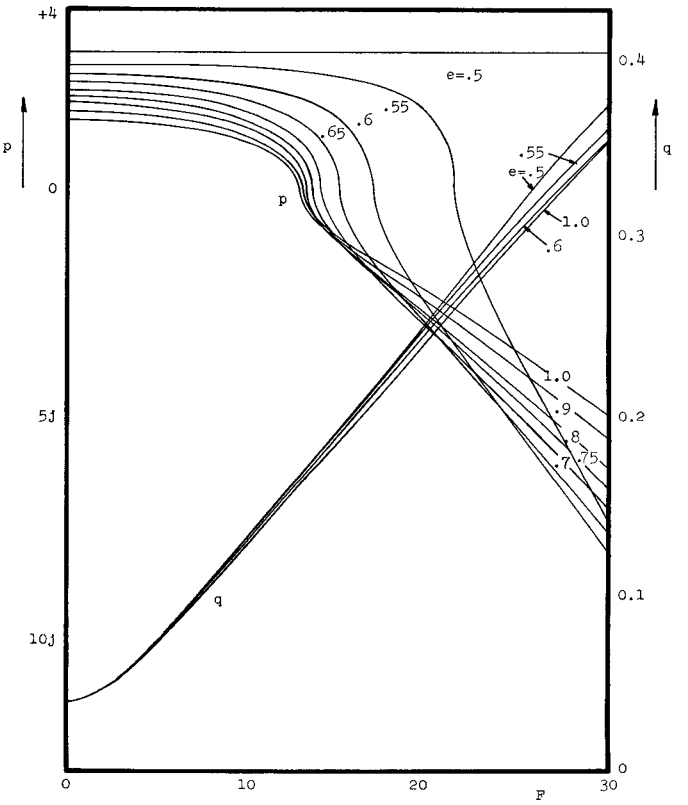

Fig. 10. p and q as a function of F and e; $c/a=0.025$.

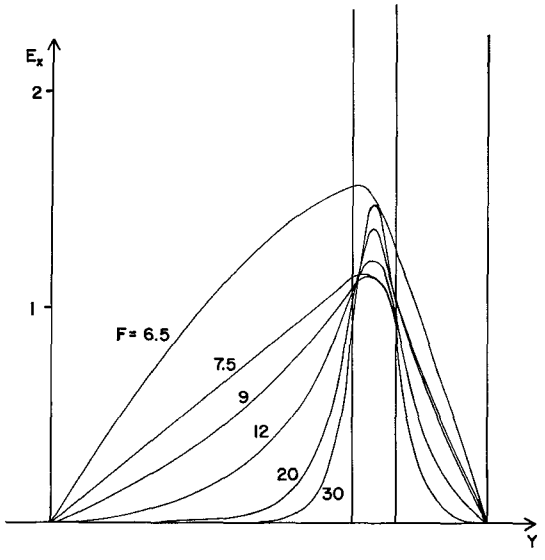

Fig. 11. Distorted TE_{10}-mode, $\epsilon=9.3$.

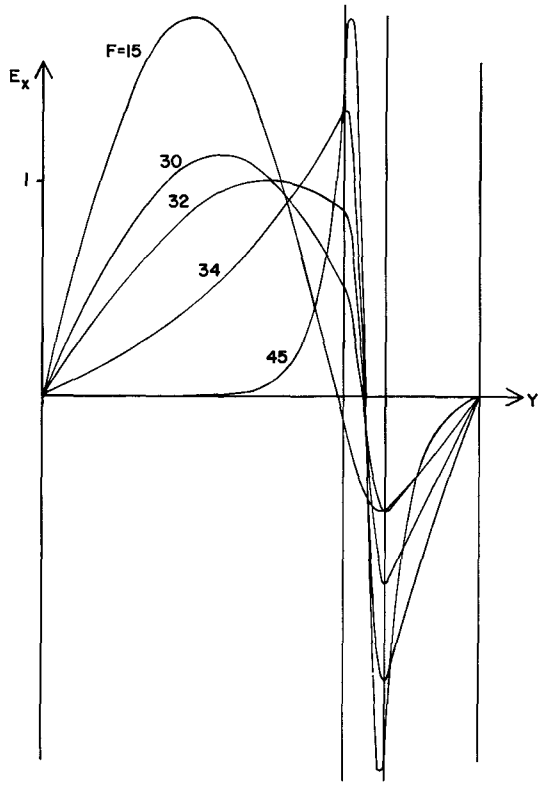

Fig. 12. Distorted TE_{20}-mode, $\epsilon=9.3$.

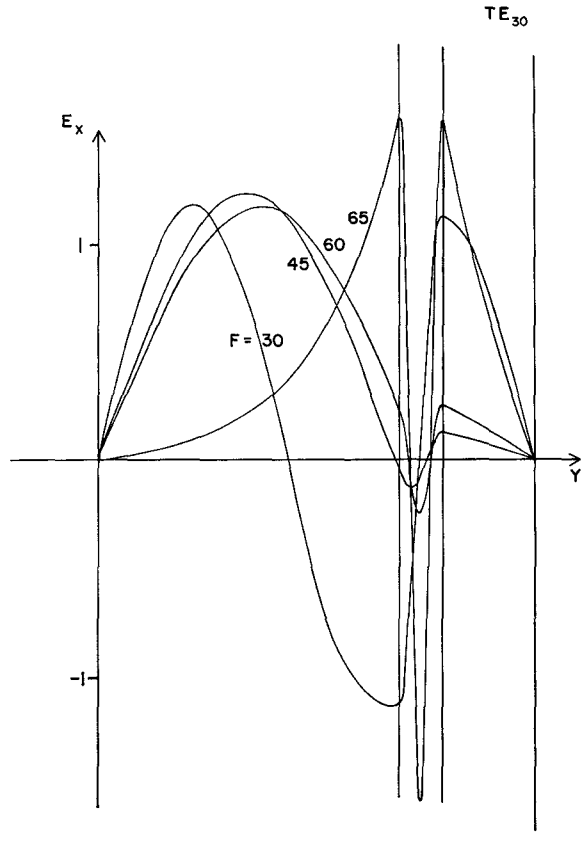

Fig. 13. Distorted TE_{30}-mode, $\epsilon=9.3$.

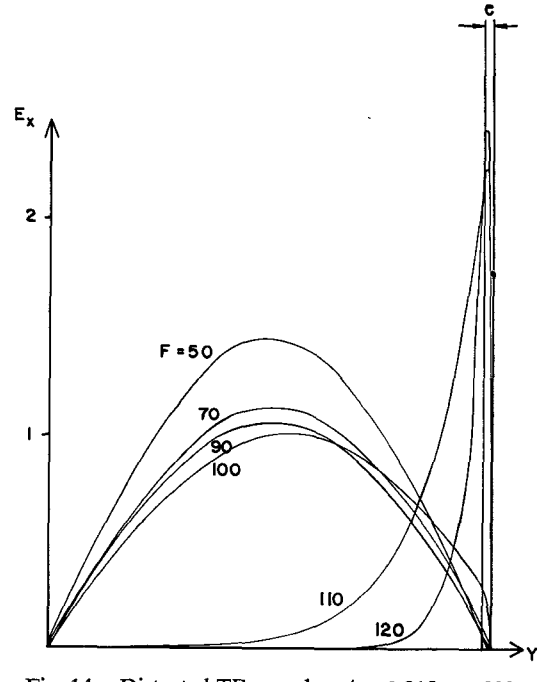

Fig. 14. Distorted TE_{10}-mode, $c/a=0.015$; $\epsilon=200$.

Summary

Solutions of the rigorous field theoretical approach to TE-modes in full height dielectrically loaded rectangular waveguides have been obtained. Numerical data about the three lowest cutoff points for $\epsilon = 9.3$ were plotted. A graphical method to determine the cutoff frequencies at other dielectric constants was developed. Using the values of the basic parameters p and q from Figs. 8 through 10 all possible information about the wave solution can be obtained for three different slab thicknesses.

Some characteristic mode patterns are presented and a physical explanation of their frequency dependence is given. With this knowledge it was possible to suggest two new applications of such waveguides.

Appendix I

According to (1) all fields are determined except to a common multiplier. This multiplier varies arbitrarily from one solution to another. In order to be able to compare different field solutions in a common scale they have to be normalized to the same total power flow P. The field strength E_x' is proportional to $\sqrt{P}$. Thus, a useful normalized field strength would be $E_x = E_x'/(g\sqrt{P})$, where g is an arbitrary constant.

Integration of Poynting's vector over the cross section of the waveguide yields

$$P = \frac{ab}{4\eta}\sqrt{\epsilon - \left(\frac{2qa}{Fc}\right)^2}(\epsilon - 1)\cdot A$$

where

$$A = \frac{2}{a}\int_0^a |E_x|^2 dy = \frac{d}{a}\left[1 - \frac{\sin 2p}{2p} + B^2\left(2e - 1 - \frac{\sin 2p(2e-1)}{2p}\right)\right] + \frac{c}{a}\left[C^2 + D^2 + \frac{(C^2 - D^2)\left(\sin 2q\left(\frac{1}{er} + 2\right) - \sin\frac{2q}{er}\right)}{4q} - CD\,\frac{\cos 2q\left(\frac{1}{er} + 2\right) - \cos\frac{2q}{er}}{2q}\right].$$

For convenience g is selected to be

$$g = \frac{4\eta}{ab}.$$

Equation (12) is the immediate result.

Appendix II

The dielectric modes can be exactly described in terms of two plane TEM-waves which are reflected back and forth between the dielectric air interfaces and have the E-field parallel to those surfaces. Compare for instance the similar approach to ordinary rectangular waveguides in Montgomery, Dicke, and Purcell [6]. At cutoff the angle of incidence upon the interface θ_i is zero (perpendicular incidence). With increasing frequency, θ_i increases quickly, passes the critical angle of total reflection, and goes to 90° if the frequency approaches infinity.

The critical angle is determined by the dielectric constant

$$\sin\theta_{crit} = \sqrt{\frac{1}{\epsilon}}.$$

For $\epsilon = 200$ the critical angle practically appears at the cutoff point.

The field strength at the interfaces is determined by the reflection coefficient for those plane waves

$$\Gamma = \frac{\eta_2\cos\theta_i - \eta_1\sqrt{1 - \epsilon\sin^2\theta_i}}{\eta_2\cos\theta_i + \eta_1\sqrt{1 - \epsilon\sin^2\theta_i}}$$

where η_1 and η_2 are the intrinsic impedances in the dielectric slab and in air.

It can easily be seen that $\Gamma \approx 1$, for $\theta_i = 0 \approx \theta_{crit}$. So indeed the interface acts as an open circuit for TEM-waves. At higher frequencies, respectively, larger θ_i, Γ passes complex values and ends up at $\Gamma = -1$, if $\theta_i \to 90°$. Consequently at high frequencies the interfaces act as short circuits.

Well above the critical frequency the reactive field outside of the slab decays very quickly. One would expect that here the solution becomes identical with the wave in a free slab of infinite height or with the wave in a slab with an infinite metal plane against one surface.

References

[1] P. H. Vartanian, W. P. Ayres, and A. L. Helgesson, "Propagation in dielectric slab loaded rectangular waveguide," *IRE Trans. on Microwave Theory and Techniques*, vol. MTT-6, pp. 215–222, April 1958.

[2] A. A. Levins, *Nomography*, 2nd ed. New York: Wiley, 1959.

[3] N. H. Frank, *Waveguide Handbook*. Cambridge, Mass.: M.I.T. Rad. Lab., 1942, Rept. 9.

[4] L. Pincherle, "Electromagnetic waves in metal tubes filled with L longitudinally with two dielectrics," *Phys. Rev.*, vol. 66, pp. 118–130, September 1944.

[5] A. D. Berk, "Variational principles for electromagnetic resonators and waveguides," *IRE Trans. on Antennas and Propagation*, vol. AP-4, pp. 104–111, April 1956.

[6] C. G. Montgomery, R. H. Dicke, and E. M. Purcell, *Principles of Microwave Circuits*, M.I.T. Rad. Lab. Series, vol. 8. New York: McGraw-Hill, 1948.

[7] L. Lewin, *Advanced Theory of Waveguides*. London: Iliffe, 1951, p. 147.

[8] N. Marcuvitz, Ed., *Waveguide Handbook*, M.I.T. Rad. Lab. Series, vol. 10. New York: McGraw-Hill, 1951, p. 389.

[9] N. Eberhardt, "The field displacement filter—a new family of dissipative waveguide filters," presented at the IEEE Internat'l Microwave Symp., Palo Alto, Calif., May 16–19, 1966 (to be published).